Applied Energy 93 (2012) 319–326

Contents lists available at SciVerse ScienceDirect

Applied Energy

journal homepage: www.elsevier.com/locate/apenergy

Real-time prediction models for output power and efficiency of grid-connected solar photovoltaic systems

Yan Su [a,*], Lai-Cheong Chan [a], Lianjie Shu [b], Kwok-Leung Tsui [c]

[a] Department of Electromechanical Engineering, University of Macau, Taipa, Macau
[b] Faculty of Business Administration, University of Macau, Taipa, Macau
[c] School of Industrial and Systems Engineering, Georgia Institute of Technology, USA

ARTICLE INFO

Article history:
Received 4 September 2011
Received in revised form 30 November 2011
Accepted 12 December 2011
Available online 4 January 2012

Keywords:
Grid connection
Solar irradiance
Photovoltaic system
Efficiency

ABSTRACT

This paper develops new real time prediction models for output power and energy efficiency of solar photovoltaic (PV) systems. These models were validated using measured data of a grid-connected solar PV system in Macau. Both time frames based on yearly average and monthly average are considered. It is shown that the prediction model for the yearly/monthly average of the minutely output power fits the measured data very well with high value of R^2. The online prediction model for system efficiency is based on the ratio of the predicted output power to the predicted solar irradiance. This ratio model is shown to be able to fit the intermediate phase (9 am to 4 pm) very well but not accurate for the growth and decay phases where the system efficiency is near zero. However, it can still serve as a useful purpose for practitioners as most PV systems work in the most efficient manner over this period. It is shown that the maximum monthly average minutely efficiency varies over a small range of 10.81% to 12.63% in different months with slightly higher efficiency in winter months.

1. Introduction

As solar energy is available in abundance most of the daytime, it is deemed to be a reliable source of renewable energy. The solar photovoltaic (PV) system that converts solar energy into electricity has become one of the most promising renewable energy systems. Its compounded growth rate is over 15% per annum in the last two decades [1,2]. Although a PV system is able to operate alone, it is frequently combined with conventional grid electricity to improve the reliability of the overall electricity generation system. The grid could provide a source of power back-up if the PV system fails to meet the load requirement.

The performance of a solar PV system is related to environmental conditions and PV system parameters. The output power generated from a solar PV system highly depends on the amount of solar radiation absorbed by the solar cells on a PV module. Due to variations of the sun's position each day and the apparent motion of the sun throughout the year, the total irradiation received at a particular site is different from time to time. Therefore, the output power of a PV system will vary with time. In addition to the inherent factor due to the sun's position/motion, other known factors affecting performance include ambient temperature, cell temperature, and local climate conditions [3].

Measured data can give realistic performance of a PV system under actual operating environments. Many authors have performed statistical analysis of energy related performance of PV systems for different purposes. For example, So et al. [4] evaluated the performance of a PV system in Korea not only for component perspective (PV array, power conditioning unit) but also for global perspective (system efficiency, energy output). Perpinan [5] studied the statistical performance of a two-axis tracking PV system for detecting malfunctioning parts of the underlying system. Ueda et al. [6] studied effects of various system configurations on the performance of grid-connected PV systems. Ayompe et al. [7] compared the efficiency of the PV system in Ireland with that in other countries. Li et al. [8] studied the performance of a PV system from both economic and environmental points of view for providing novel findings on the promotion of PV systems.

In addition to the statistical analysis of PV systems, interest in forecasting PV performance like solar power and system efficiency has increased in recent years. Many of these consider forecasts of the global irradiance which can be viewed as a problem similar to that of forecasting solar power. This is because the estimate of global irradiance can provide a rough estimate of the aggregate energy produced by the solar panels connected to the grid. A sample of research on forecasting solar irradiance includes [9–18]. In theory, the above approaches to prediction of global irradiance can be applied to the prediction of solar power. However, there is significantly less research predicting the actual output of PV systems.

* Corresponding author.
E-mail address: yansu@umac.mo (Y. Su).

0306-2619/$ - see front matter © 2011 Elsevier Ltd. All rights reserved.
doi:10.1016/j.apenergy.2011.12.052

Nomenclature

t	time period	$\overline{R}_y(t)$	yearly average minutely solar irradiance
d	day	$\overline{R}_m(t)$	monthly average minutely solar irradiance
N_y	number of days in a year	$\widehat{\overline{R}}_y(t)$	fitted value of $\overline{R}_y(t)$
N_m	number of days in a month	$\widehat{\overline{R}}_m(t)$	fitted value of $\overline{R}_m(t)$
P_{td}	output power at time t in day d	η_{td}	PV system efficiency at time t in day d
$\overline{P}_y(t)$	yearly average minutely output power	$\bar{\eta}_y(t)$	yearly average minutely system efficiency
$\overline{P}_m(t)$	monthly average minutely output power	$\bar{\eta}_m(t)$	monthly average minutely system efficiency
$\widehat{\overline{P}}_y(t)$	fitted value of $\overline{P}_y(t)$	$\hat{\bar{\eta}}_y(t)$	fitted value of $\bar{\eta}_y(t)$
$\widehat{\overline{P}}_m(t)$	fitted value of $\overline{P}_m(t)$	$\hat{\bar{\eta}}_m(t)$	fitted value of $\bar{\eta}_m(t)$
A	estimate of peak parameter for the Gaussian model	$\hat{\bar{\eta}}^*_m(t)$	maximum of $\hat{\bar{\eta}}_m(t)$
μ	estimate of mean for the Gaussian model	R^2	coefficient of determination
σ	estimate of standard deviation for the Gaussian model	*RMSE*	root mean square error
R_{td}	solar irradiance at time t in day d		

The models for predicting PV performance can be generally classified into three categories: physics-based models, time series models, and models based on neural networks (NN). The first category aims at developing mathematical models of the PV performance as a function of some independent variables, including the characteristic parameters of PV module, solar radiation, ambient temperature, and wind speed. These mathematical models are often derived based on physical properties of individual components in the PV system (e.g., the PV cell/module, the battery, the inverter). For example, there are some PV-cell efficiency models expressed as being dependent on the solar radiation and cell temperature [19–21]. Ayompe et al. [22] compared the prediction accuracy of PV output power by using different models for PV-cell temperature and models for PV-cell efficiency. Based on the equivalent circuit of a one diode-model, the four and five-parameter models were also investigated [23–26] and compared [27]. These parametric models consider the most important characteristics parameters, i.e., the short-circuit current, open-circuit voltage, and maximum power output of the PV module. In addition, based on an adaption of the established fill factor (FF) method, Jones and Underwood [28] proposed a more general efficiency model of PV module power output with the consideration of solar radiation and module temperature characteristics. Note that there appear to be many parameters required to be specified in these physics-based models, which are normally unavailable and often determined based on simulations.

Statistical forecasting of solar data using time series model has been well established since the pioneering work of Goh and Tan [29]. For example, Bacher et al. [30] described a two-state method for predicting the aggregate solar power, where the clear sky model approach was first used to normalize solar power and then an adaptive time series model was applied for prediction. A more complicated approach is to use NNs to predict the energy output by using different inputs such as the solar radiation, ambient temperature, and module temperature, see, for example, [31–33]. However, the design of NN models heavily relies on past experience and is subject to trial and error processes.

Most of the models like the time series models in the above cited papers for assessing the PV system performance are lumped in the sense that they determine average daily, monthly or annual energy output. These lump models are useful for predicting the future daily/monthly/annual output; however, they are not adapted to analyze the real-time or intra-day dynamic performance of PV systems. The intra-day dynamic pattern provides valuable on-line information for designers and users for analyzing the performance of their solar PV system. For example, designers can know when the PV system provides electricity less than the load demand by analyzing the changing pattern of the energy output. It would be cost effective when there is a good match between the utility load and the solar resource profile [34]. Additionally, the physics-based models need to specify many parameters and some parameters are normally unavailable in practice. The NN models have complicated structures. These limitations cannot lead to easy manipulation of the system performance. Therefore, a simple model with acceptable accuracy would be desirable for real-time prediction of PV system performance.

The objective of this paper is to present a simple but accurate on-line estimation model of solar PV system output as well as an on-line estimation model for the corresponding efficiency. The proposed models are based on Gaussian equations, which require less computational efforts in model structure identification and parameter estimation as compared to the existing models. Therefore, they are simple to implement in practice. Moreover, the proposed models are shown to be able to estimate the PV system performance with reasonable accuracy, which will be validated based on measured data of a grid connected PV system in Macau.

2. The grid-connected PV system in Macau

The grid-connected PV system for the present study was mounted on the rooftop of an institutional building. The institution is located in a low density area, the Coloane island of Macau Special Administrative Region (SAR) (latitude = 22°10′0″N and longitude = 113°33′0″E). The underlying PV system consists of twelve Kyocera HTS-175 modules covering a total area of 15.325 m^2 (12 pcs × 1.29 m × 0.99 m) with an installed capacity of 2.1 kW. Under standard test conditions (i.e., cell temperature = 25 °C, solar irradiance = 1 kW/m^2), the maximum output power of the HTS-175 module is 175 W ± 5%, as stated in the product catalogue. Each of the modules comprises 48 solar cells made of multi-crystalline silicon wafers. The PV module specifications are shown in Table 1. In general, inclined modules can prevent accumulation of dust on the surface and provide a natural cooling effect. The PV modules were installed of an inclination angle of 10°, facing south-east.

A single Xantrex^{TM} grid tie (GT series) solar inverter was used to convert DC to AC. Under AC output voltage of 240 V, this inverter

Table 1
PV module specifications.

PV module	Specification
Type	HTS-175
Maximum power	175 W
Maximum power voltage	24.3 V
Maximum power current	7.2 A
Open circuit voltage	29.3 V
Short circuit current	7.9 A

can provide maximum continuous output current of 11.7A. The maximum AC power output is 2.8 kW for the electrical input. This inverter has MPPT operating range from 193 Vdc to 550 Vdc with the maximum input current of 15.4 Adc. The maximum inverter efficiency is 95%. Power generated from the PV system was fed directly into the grid of a local power company. The PV system was automatically connected to the electrical grid at 5 am and disconnected at 8 pm each day. The energy output data as well as measurements of solar irradiance, ambient temperature and wind speed were recorded by a data logger at an interval of 1 min.

The PV system was launched in late June 2010, the output energy and solar radiation data recorded during the 12-month period from July 2010 to June 2011 were used for the study. It is inevitable that there were some missing data for various reasons such as instrument malfunction and maintenance. Both the output power and system efficiency are the two most important measures of performance for a PV system. In what follows, we discuss the real time prediction models for the output power and corresponding efficiency of the underlying PV system.

3. The prediction model for output power

The 1-min readings of output power in the data set can be arranged in matrix form. Let P_{td} represent the measured output power per unit area at time t in the day d. Since some values were not available, some elements in the matrix were empty. Different classes of time averages can be computed, depending on the time frame (e.g., one month/quarter/year) to be considered. In this paper, we considered two types of time averages while the other classes of time averages can be similarly discussed, including both the yearly average and the monthly average of 1-min readings. Let N_y (or N_d) be the number of days during the one-year (or one-month) time period. Then the yearly and monthly averages of the 1-min readings of output power at time t can be computed by

$$\overline{P}_y(t) = \frac{1}{N_y}\sum_{d=1}^{N_y} P_{td}$$

and

$$\overline{P}_m(t) = \frac{1}{N_m}\sum_{d=1}^{N_m} P_{td},$$

respectively.

The instantaneous output power generated by the PV system will be changing with time as the solar radiation absorbed by PV cells varies from morning to night. Fig. 1 depicts the daily profiles of output power generated from the PV system during four days from March 4 to March 7, 2011. These four days were chosen to cover the changing weather patterns as widely as possible. March 4 and March 7 were clear days, March 5 was heavily overcast, and March 6 was slightly cloud covered. During days with heavily overcast sky and slight cloud covered sky, the output power shows an irregular profile. During clear days, the output power shows a similar profile that seems to be bell shaped.

Fig. 2a and b show plots of the annual and monthly averages of the minutely output power, respectively. From Fig. 2a, the yearly average of the 1-min output power crosses the zero line at 6:22 in the early morning and then starts to increase, reaching the peak at noon time, say 12:30. It then starts to decrease and declines to zero at 18:35 in the evening. Outside the time interval [6:22, 18:35], the mean energy output is zero. This observation indicates that the more efficient operation time of the current system is from 06:22 to 18:35 in order to generate positive output power, although it currently operates during the time period from 5 am to 8 pm each day.

Fig. 2b plots the monthly averages of the 1-min output power in a winter month (January) and in a summer month (July). At the same time period, the $\overline{P}_m(t)$ value in July tends to be higher than that in January as expected. The highest value of $\overline{P}_m(t)$ in July was around 65 W/m^2 at 12:30 while that in January was around 55 W/m^2 at 12:45. Moreover, the value of $\overline{P}_m(t)$ approaches zero in July outside the time interval [6:22, 18:35] while that approaches zero in January outside the time interval [7:22, 17:55]. This indicates that the length of period of the underlying PV system to generate positive $\overline{P}_m(t)$ value is longer in a summer day than in a winter day.

A pronounced observation from Fig. 2a and b is that the yearly/monthly means of the minutely output power can be well fitted with a bell-shaped curve. According to the central limit theorem (CLT), the distribution of sample mean can be well approximated by a Gaussian/normal distribution when the sample size is sufficiently large, independent of the population distribution. This motivates us to use a Gaussian curve to fit the output power data. The Gaussian distribution is one of the most common distributions in nature. The need to fit a Gaussian curve to experimental data is numerous and appears in all the physical, biological, and ecological settings [35–37].

3.1. Prediction of the annual mean minutely output power

The Gaussian equation for fitting the annual mean minutely output power has the form

$$\widehat{\overline{P}}_y(t) = \frac{A}{\sigma\sqrt{2\pi}}\exp\left[-\frac{(t-\mu)^2}{2\sigma^2}\right] \quad (1)$$

where $\widehat{\overline{P}}_y(t)$ denotes the estimated value of $\overline{P}_y(t)$, and μ, σ and A represent the estimated values of the three parameters of Gaussian equation. In particular, μindicates the time at which $\widehat{\overline{P}}_y(t)$ peaks, σ is the standard deviation of time in the unit of minutes, and

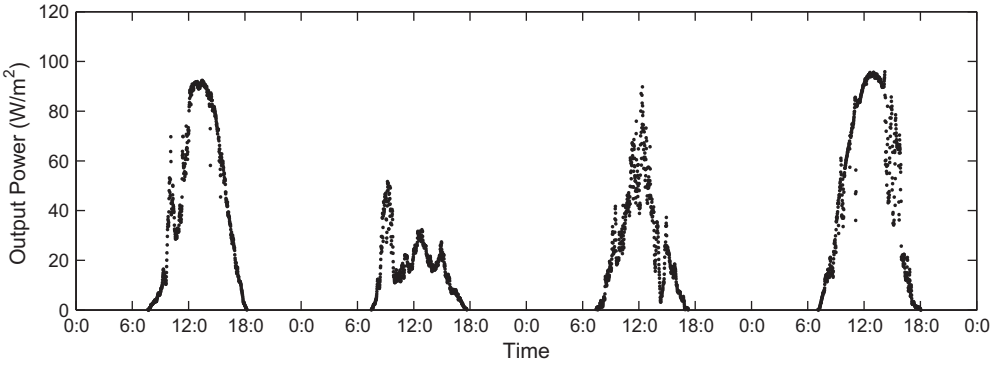

Fig. 1. The daily profiles of output power generated from the PV system during the four days from March 4 to March 7, 2011.

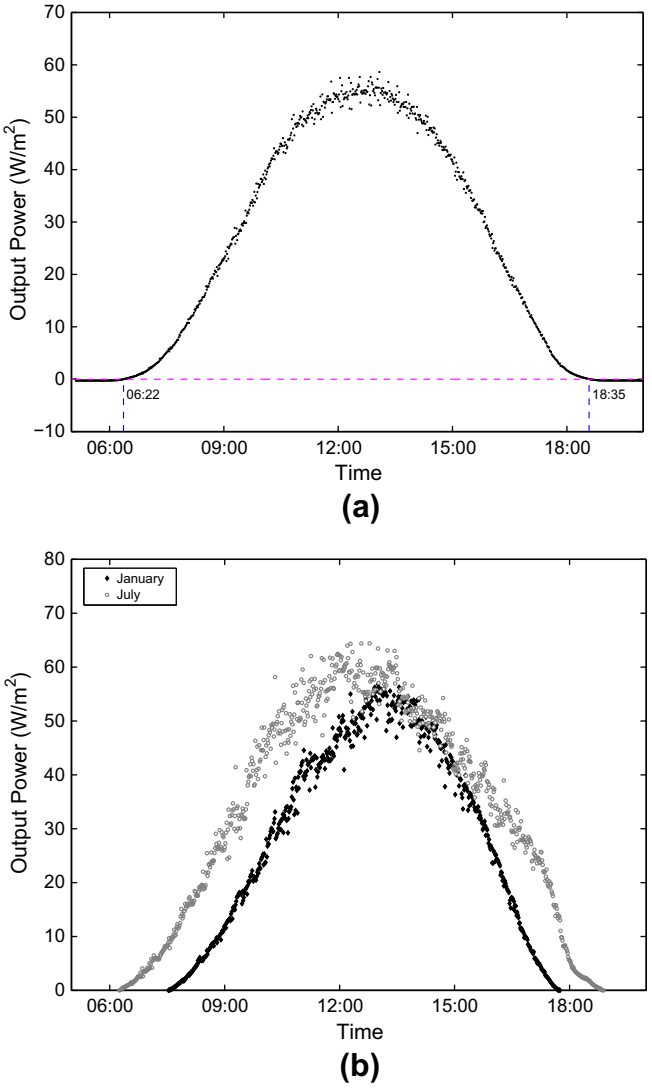

Fig. 2. (a) Yearly and (b) monthly averages of the minutely output power.

$A/\left(\sigma\sqrt{2\pi}\right)$ is the maximum of the Gaussian curve. In order to obtain the three estimates, μ, σ and A, the recursive least squares method can be used to minimize the root mean squared error (RMSE) as

$$RMSE = \sqrt{\frac{1}{N}\sum_{i=1}^{N}\left(\widehat{\overline{P}}_y(t) - \overline{P}_y(t)\right)^2}$$

Based on the data set with N_y points $(t, \overline{P}_y(t))$, the three Gaussian parameters in Eq. (1) were estimated as

$$A = 2.296 \times 10^4, \quad \mu = 12:38, \quad and \quad \sigma = 157.8, \tag{2}$$

with R^2 = 97.96%. The value of R^2, known as coefficient of determination, is a convenient statistic parameter to measure how well the regression curve fits the data. It represents the percentage of the total variance accounted for by the fitted curve. The high value R^2 = 97.96% indicates that around 97.96% of the total variation in $\overline{P}_y(t)$ can be explained by the Gaussian model and only 2.04% left unaccounted for.

3.2. Prediction of the monthly mean minutely output power

Due to the variation in solar irradiance each month, the average output power generated from a solar PV system varies from month to month, as can also be seen from Fig. 2b. In order to take the month-to-month variation into account, one can fit the Gaussian curve to the monthly average minutely output power. Likewise, the corresponding Gaussian equation can be defined as

$$\widehat{\overline{P}}_m(t) = \frac{A}{\sigma\sqrt{2\pi}} \exp\left[-\frac{(t-\mu)^2}{2\sigma^2}\right],$$

where $\widehat{\overline{P}}_m(t)$ stands for the fitted value of $\overline{P}_m(t)$, and μ, σ, and A are the respective estimates when the Gaussian curve was fit to the data points $(t, \overline{P}_m(t))$.

Table 2 summarizes the estimated Gaussian parameters as well as the R^2 value. It is not surprising to see that the highest A occurs in July ($A = 2.7670 \times 10^4$) and the lowest occurs in February ($A = 1.5497 \times 10^4$). In summer (June, July, August), the value of A ranges between 2.6939×10^4 and 2.7670×10^4, and in winter (December, January, February), the value of A ranges between 1.5479×10^4 and 1.9068×10^4.

Moreover, note that the coefficient of determination, R^2, of the fitted curve varies from month to month. The lowest R^2 value is 91.33% in April, and the highest is 97.22% in March. However, all the coefficients of determination are relatively high, indicating that the above fit is sufficient for practical use.

4. The prediction model for system efficiency

The transient system energy efficiency at any date and time is defined as the ratio of the output power to the solar irradiance per unit area of the PV plates, i.e.,

$$\eta_{td} = \frac{P_{td}}{R_{td}} \tag{3}$$

As there is a strong relationship between output power and solar irradiance, the dynamic pattern of the solar irradiance can also be well fitted using the Gaussian curve. As a result, the online system efficiency can be estimated based on Eq. (3) once the prediction models for the output power and solar irradiance are established. In the following, we first discuss the prediction model for solar irradiance before discussing the prediction model for system efficiency.

4.1. The prediction model for solar irradiance

Likewise, the daily profiles of solar irradiance measured during the four days from March 4 to March 7, 2011 are plotted in Fig. 3. Similar trends to those in Fig. 1 can be observed. The maximum solar irradiance received at noon on a clear day is around 800 W/m^2. On March 5 with heavily overcast sky, the solar irradiance exhibits an irregular profile.

Table 2
Estimated Gaussian parameters based on the monthly average minutely output power.

Month	A ($\times 10^4$)	μ	σ	R^2
2010/7	2.7670	12:43	171.4	0.9474
2010/8	2.7285	12:50	171.1	0.9426
2010/9	2.5318	12:36	165.7	0.9639
2010/10	2.5062	12:21	146.7	0.9708
2010/11	2.2960	12:28	142.9	0.9644
2010/12	1.8026	12:40	138.1	0.9701
2011/01	1.9068	13:03	137.9	0.9714
2011/02	1.5497	12:41	148.0	0.9492
2011/03	1.9442	12:44	147.6	0.9722
2011/04	2.7160	12:50	141.5	0.9133
2011/05	2.5122	12:19	162.4	0.9424
2011/06	2.6939	12:32	164.5	0.9519

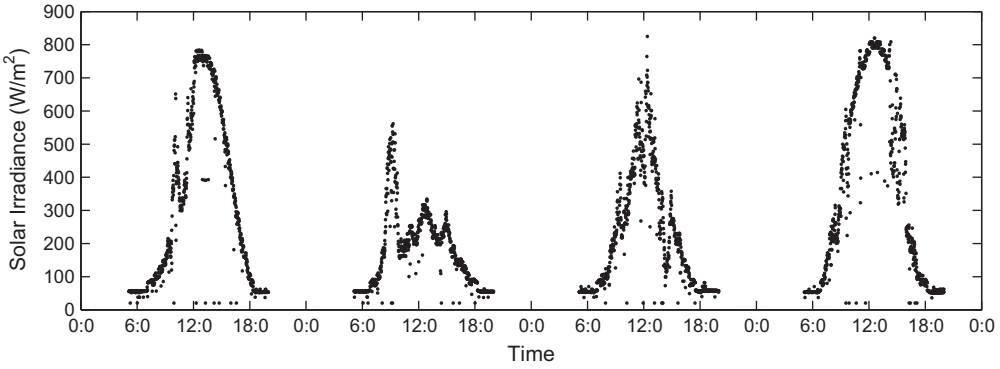

Fig. 3. The daily profiles of solar irradiance measured during the four days from March 4 to March 7, 2011.

The yearly and monthly averages of the minutely solar irradiance are further plotted in Fig. 4a and b, respectively. By comparing Figs. 3 and 4 with Figs. 1 and 2, it is straightforward that the solar irradiance exhibit a pattern very similar to the output power. After all, the output power and solar irradiance are highly correlated. This in turn implies that the Gaussian model is sufficient to characterize the varying pattern of solar irradiance.

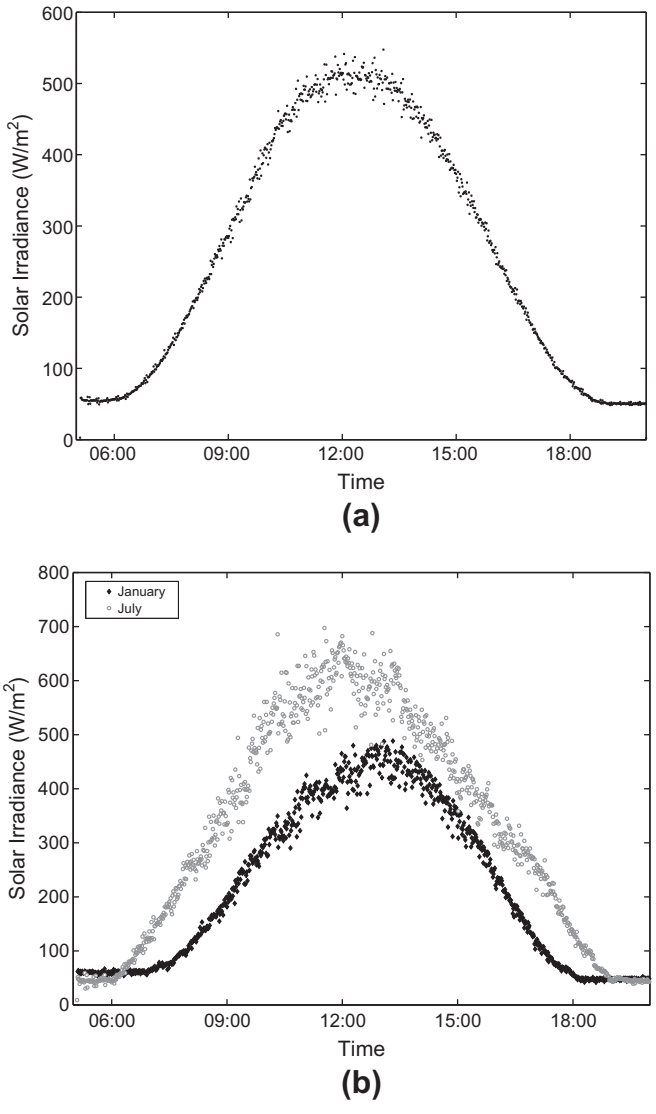

Fig. 4. (a) Yearly and (b) monthly averages of the minutely solar irradiance.

Analogously, one can define the yearly and monthly averages of the 1-min readings of solar irradiance at time t as

$$\overline{R}_y(t) = \frac{1}{N_y}\sum_{d=1}^{N_y} R_{td}$$

and

$$\overline{R}_m(t) = \frac{1}{N_m}\sum_{d=1}^{N_m} R_{td},$$

respectively, where R_{td} represent the measured solar irradiance at time t in the day d. By performing Gaussian fit of $\overline{R}_y(t)$ on time t, the resulting prediction equation was obtained as

$$\widehat{\overline{R}}_y(t) = \frac{2.2864\times 10^5}{174.9\sqrt{2\pi}}\exp\left[-\frac{(t-12:22)^2}{2\times(174.9)^2}\right], \quad (4)$$

where $\widehat{\overline{R}}_y(t)$ denotes the fitted value of $\overline{R}_y(t)$. The corresponding R^2 value is $R^2 = 98.65\%$, indicating an excellent fit of the Gaussian curve to the data $(t, \overline{R}_y(t))$.

Comparing Eq. (4) with Eq. (2), it is interesting to observe that the yearly average minutely solar irradiance peaks at $\mu = 12{:}22$, which is 16 min earlier than that of the yearly average minutely output power ($\mu = 12{:}38$). This is reasonable because there exist some transient delays in a PV system before the solar irradiance is transformed into output power. Moreover, notice that the estimated standard deviation based on the yearly solar irradiance ($\sigma = 174.9$) is about 17 min larger than that based on the yearly output power ($\sigma = 157.8$).

Table 3 summarizes the estimated parameters when the Gaussian curve was fitted to the monthly average minutely solar irradiance data, $(t, \overline{R}_m(t))$, along with the resulting R^2 value. Similar to the observations in Table 2, it can be seen that the summer months

Table 3
Estimated Gaussian parameters based on the monthly average minutely solar irradiance.

Month	A ($\times 10^5$)	μ	σ	R^2
2010/07	2.8496	12:21	185.9	0.9560
2010/08	2.6515	12:33	182.2	0.9487
2010/09	2.4959	12:18	177.9	0.9605
2010/10	2.4241	12:08	162.6	0.9693
2010/11	2.1465	12:10	159.2	0.9591
2010/12	1.7533	12:23	156.0	0.9614
2011/01	1.7884	12:45	159.3	0.9542
2011/02	1.6111	12:22	170.8	0.9285
2011/03	1.9081	12:36	169.1	0.9657
2011/04	2.7473	12:35	159.8	0.9137
2011/05	2.6334	12:05	178.0	0.9406
2011/06	2.8495	12:15	182.2	0.9358

like June and July generate relatively high values of A, and the winter months like January and February generate relatively low values of A. This result is consistent with that observed in [38,39]. Another sounding observation from Table 3 is that for a given month, the prediction model for $\overline{R}_m(t)$ has smaller μ value but larger σ value, as compared to the prediction model for $\overline{P}_m(t)$ shown in Table 2.

4.2. Prediction of yearly and monthly mean minutely system efficiency

Based on Eqs. (4) and (2), the prediction model for the yearly average minutely efficiency can be expressed as

$$\hat{\bar{\eta}}_y(t) = \frac{\hat{\overline{P}}_y(t)}{\hat{\overline{R}}_y(t)} = 0.1113 \exp\left[\frac{(t-12:38)^2}{2\times(157.8)^2} - \frac{(t-12:22)^2}{2\times(174.9)^2}\right]. \quad (5)$$

The derivative of $\hat{\bar{\eta}}_y(t)$ with respect to time t is given by

$$\frac{d}{dt}[\hat{\bar{\eta}}_y(t)] = \hat{\bar{\eta}}_y(t)\left[\frac{(t-12:38)}{(157.8)^2} - \frac{(t-12:22)}{(174.9)^2}\right].$$

When $d[\hat{\bar{\eta}}_y(t)]/dt = 0,\ t = 13:38$. That is, the yearly mean minutely energy efficiency reaching the maximum was estimated to be at time t = 13:38.

To get some visual insights into the curve in Eq. (5), Fig. 5 plots the fitted yearly average minutely efficiency ($\hat{\bar{\eta}}_y(t)$) as well as the measured value ($\bar{\eta}_y(t)$). It is interesting to note that the system efficiency of a PV system is often relatively low. For the underlying PV system in Macau, the yearly average system efficiency is less than 12%. Moreover, from Fig. 5, one can approximately divide the dynamic pattern of system efficiency into three phases: the growth phase over the period from 6 am to 9 am, the intermediate phase from 9 am to 4 pm, and the decay phase from 4 pm to 6:35 pm. In the growth phase, the system efficiency quickly increases to a relatively high value, starting from zero at 6 am. Over the intermediate period from 9 am to 4 pm, the system efficiency remains at a relatively high level, which varies within a small range [8%, 11.5%]. After 4 pm in the afternoon, the system efficiency quickly decreases from a relatively high level and decays to zero around 6:35 pm. This varying pattern is due to variations in the sun's position each day, which results in different irradiation received at a particular site. As a result, the system efficiency exhibits a three-phase changing pattern within a day.

A pronounced observation from Fig. 5 is that the curve in Eq. (5) fits the data very well over the intermediate period but not for the growth and decay phases. There exists large discrepancy between the predicted and measured yearly averages of the minutely system efficiency during these two phases, especially at the starting period and the ending period when the system efficiency is close to zero. This is because Gaussian functions can never reach zero, while real output power and solar irradiance are measured to be zero at early morning and night. The division by a nearly zero irradiance could cause great errors in the estimation of system efficiency. In practice; however, practitioners are more interested in the time period with relatively high system efficiency. Therefore, the model in Eq. (5) can serve a useful purpose for the real time prediction of energy efficiency for a solar PV system although it is not accurate for the growth and decay phases.

Table 4 summarizes the prediction model for the monthly average minutely system efficiency. The maximum value of $\hat{\bar{\eta}}_m(t),\ \hat{\bar{\eta}}^*_m(t)$, is given by the last column of Table 4. It is interesting to observe that $\hat{\bar{\eta}}^*_m(t)$ is 12.63% in January and 10.99% in July. This is consistent with the well-known result that the system efficiency in winter months tends to be higher than that in summer months [8,40]. This is because efficiency decreases with increases in PV cell

Table 4
The prediction model for the monthly average minutely system efficiency.

Month	Model	Extreme $(t,\ \hat{\bar{\eta}}^*_m(t))$
2010/07	$\hat{\bar{\eta}}_m(t) = 0.1053 \exp\left[\frac{(t-12:43)^2}{2\times(171.4)^2} - \frac{(t-12:21)^2}{2\times(185.9)^2}\right]$	(14:41, 10.99%)
2010/08	$\hat{\bar{\eta}}_m(t) = 0.1096 \exp\left[\frac{(t-12:50)^2}{2\times(171.1)^2} - \frac{(t-12:33)^2}{2\times(182.2)^2}\right]$	(14:56, 11.37%)
2010/09	$\hat{\bar{\eta}}_m(t) = 0.1089 \exp\left[\frac{(t-12:36)^2}{2\times(165.7)^2} - \frac{(t-12:18)^2}{2\times(177.9)^2}\right]$	(14:34, 11.32%)
2010/10	$\hat{\bar{\eta}}_m(t) = 0.1146 \exp\left[\frac{(t-12:21)^2}{2\times(146.7)^2} - \frac{(t-12:08)^2}{2\times(162.6)^2}\right]$	(13:17, 11.66%)
2010/11	$\hat{\bar{\eta}}_m(t) = 0.1189 \exp\left[\frac{(t-12:28)^2}{2\times(142.9)^2} - \frac{(t-12:10)^2}{2\times(159.2)^2}\right]$	(13:42, 12.28%)
2010/12	$\hat{\bar{\eta}}_m(t) = 0.1162 \exp\left[\frac{(t-12:40)^2}{2\times(138.1)^2} - \frac{(t-12:23)^2}{2\times(156.0)^2}\right]$	(13:41, 11.94%)
2011/01	$\hat{\bar{\eta}}_m(t) = 0.1232 \exp\left[\frac{(t-13:03)^2}{2\times(137.9)^2} - \frac{(t-12:45)^2}{2\times(159.3)^2}\right]$	(13:56, 12.63%)
2011/02	$\hat{\bar{\eta}}_m(t) = 0.1110 \exp\left[\frac{(t-12:41)^2}{2\times(148.0)^2} - \frac{(t-12:22)^2}{2\times(170.8)^2}\right]$	(13:38, 11.38%)
2011/03	$\hat{\bar{\eta}}_m(t) = 0.1167 \exp\left[\frac{(t-12:44)^2}{2\times(147.6)^2} - \frac{(t-12:36)^2}{2\times(169.1)^2}\right]$	(13:09, 11.72%)
2011/04	$\hat{\bar{\eta}}_m(t) = 0.1136 \exp\left[\frac{(t-12:50)^2}{2\times(141.5)^2} - \frac{(t-12:35)^2}{2\times(159.8)^2}\right]$	(14:02, 11.62%)
2011/05	$\hat{\bar{\eta}}_m(t) = 0.1066 \exp\left[\frac{(t-12:19)^2}{2\times(162.4)^2} - \frac{(t-12:05)^2}{2\times(178.0)^2}\right]$	(13:10, 10.81%)
2011/06	$\hat{\bar{\eta}}_m(t) = 0.1058 \exp\left[\frac{(t-12:32)^2}{2\times(164.5)^2} - \frac{(t-12:15)^2}{2\times(182.2)^2}\right]$	(14:03, 10.86%)

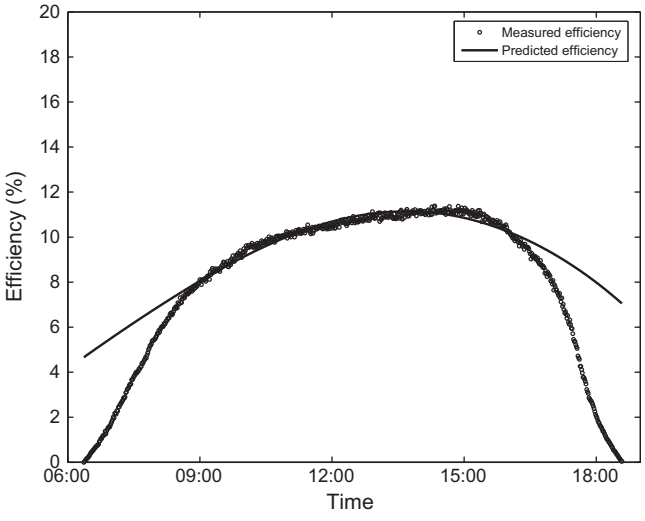

Fig. 5. Comparison of predicted and measured yearly mean minutely system efficiency.

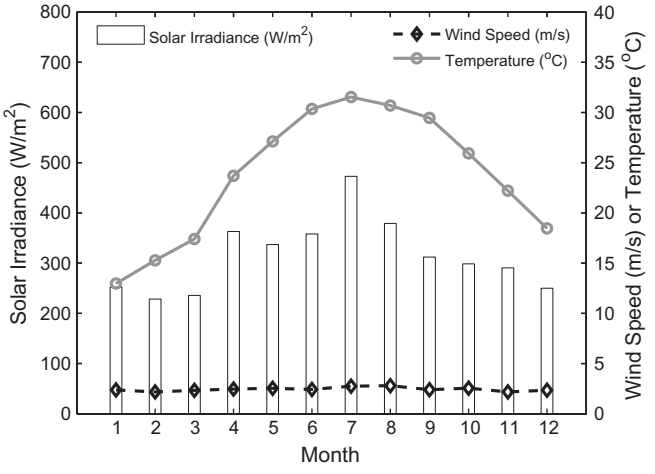

Fig. 6. Monthly average solar irradiance, ambient temperature, and wind speed.

temperature. Fig. 6 plots the monthly average ambient temperature as well as the monthly average solar irradiance and wind speed. It is clear that the mean temperature in winter month (January) is around 14 °C, which is much lower than that of 31 °C in summer month (July). Therefore, the system efficiency in winter is expected to better than that in summer.

To illustrate how well the curve fits the monthly average minutely efficiency, Fig. 7 plots the predicted and measured values of

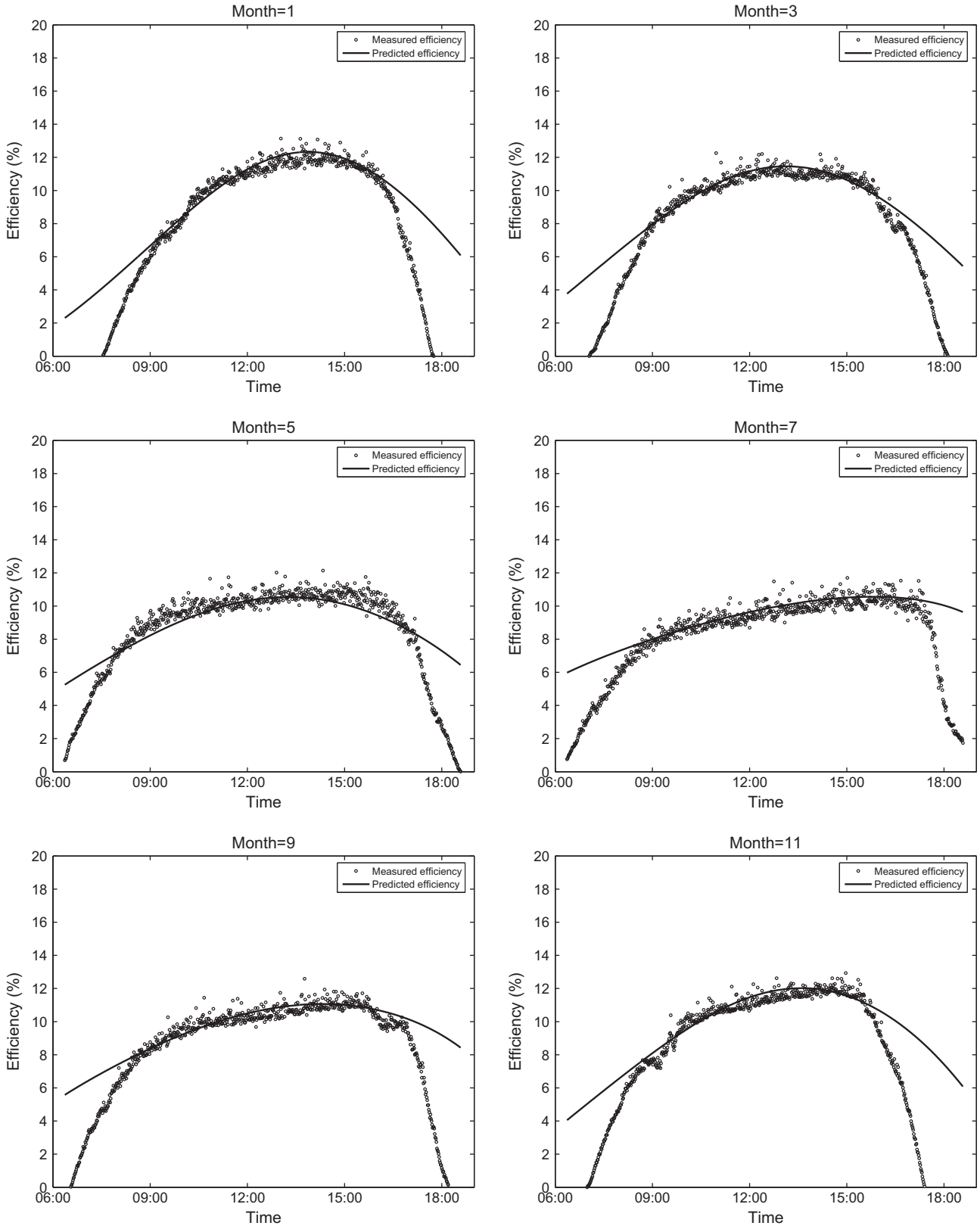

Fig. 7. Comparison of predicted and measured monthly mean minutely system efficiency.

$\bar{\eta}_m(t)$ for odd months. The monthly mean minutely system efficiency exhibits a similar pattern over all months considered here. Once again, these plots indicate that the curve fits $\bar{\eta}_m(t)$ very well during the intermediate phase but not for the growth and decay phases.

5. Conclusions

The output power and system efficiency of a solar PV system is not fixed but changes over time each day. The daily changing patterns provide valuable on-line information for designers and users for analyzing the performance of their solar PV system. The objective of this paper was to develop a real time prediction model for yearly and monthly average minutely power output as well as an on-line estimation model for system efficiency. The proposed models are based on Gaussian equations and have been validated by the measured data of a grid-connected solar PV system in Macau.

The result indicates that the yearly mean minutely energy output approaches zero before 6:22 am and after 18:35 pm. Therefore, a more efficient operation time period of the current system is from 06:22 to 18:35 in order to generate positive output power although it currently operates during the period from 5 am to 8 pm each day. The prediction model for monthly average minutely output power shows that the average output power tends to be higher in summer months than that in winter months. The value of A varies between 1.5479×10^4 and 1.9068×10^4 in winter months and varies between 2.6939×10^4 and 2.7670×10^4 in summer months.

The prediction model for solar irradiance is similar to that for output power as they are highly correlated. It is interesting to note that the solar irradiance and output power do not reach their peak value at the same time point. Rather, the peak time for solar irradiance is earlier than that for output power. For example, the yearly average minutely solar irradiance peaks at 12:22 while the yearly average minutely output power peaks at 12:38.

The ratio of the predicted output power to the predicted solar irradiance was used to predict the real time efficiency of the PV system. The resulting model fits the intermediate period (9 am to 4 pm) quite well but not for the growth and decay phases where the system efficiency is near zero. However, the period from 9 am to 4 pm represents the most important operation period for a PV system as it works in the most efficient manner during this period. The proposed prediction model can serve a useful purpose for the real time prediction of system efficiency for a solar PV system. The prediction model shows that the maximum monthly average minutely energy efficiency ranges from 10.81% to 12.63%. In general, the efficiency in winter months is better than that in summer months.

Acknowledgments

The authors would like to thank the editor and two referees for their valuable comments. Yan Su's work was supported by the Research Committee under MYRG151(Y1-L2)-FST11-SY and SRG009-FST11-YS.

References

[1] Mondal MAH, Islam AKMS. Potential and viability of grid-connected solar PV system in Bangladesh. Renew Energy 2011;36:1869–74.
[2] Green MA. Recent developments in photovoltaics. Sol Energy 2004;76:3–8.
[3] Roberts R. Electricity, hertfordshire. UK: Prentice Hall; 1991.
[4] So JH, Jung YS, Yu GJ, Choi JY, Choi JH. Performance results and analysis of 3kw grid-connected PV systems. Renew Energy 2007;32:1858–72.
[5] Perpinan O. Statistical analysis of the performance and simulation of a two-axis tracking PV system. Sol Energy 2009;83:2074–85.
[6] Ueda Y, Kurokawa K, Kitamura K, Yokota M, Akanuma K, Sugihara H. Performance analysis of various system configurations on grid-connected residential PV systems. Sol Energy Mater Sol Cells 2009;93:945–9.
[7] Ayompe LM, Duffy A, McCormack SJ, Conlon M. Measured performance of a 1.72 kW rooftop grid connected photovoltaic system. Energy Convers Manag 2011;52:816–25.
[8] Li DHW, Cheung KL, Lam KL, Chan WWH. A study of grid-connected photovoltaic (PV) system in Hong Kong. Appl Energy. doi:10.1016/j.apenergy.2011.01.054.
[9] Chowdhury B, Rahman S. Forecasting sub-hourly solar irradiance for prediction of photovoltaic output. In: IEEE photovoltaic specialists conference; 1987. p. 171–6.
[10] Sfetsos A, Coonick A. Univariate and multivariate forecasting of hourly solar radiation with artificial intelligence techniques. Sol Energy 2000;68(2):169–78.
[11] Hontoria L, Aguilera J, Zuria P. Generation of hourly irradiation synthetic series using the neural network multilayer perception. Sol Energy 2002;72:441–6.
[12] Shuanghua C, Jiacong C. Forecast of solar irradiance using recurrent neural networks combined with wavelet analysis. Appl Therm Eng 2005;25:161–72.
[13] Mellit A, Benghanem M, Kalogirou SA. An adaptive wavelet network model for forecasting daily total solar radiation. Appl Energy 2006;83:705–22.
[14] Lorenz E, Heinemann D, Wickramarathne H, Beyer H, Bofinger S. Forecast of ensemble power production by grid-connected PV systems. In: Proceedings of the 20th European PV conference, Milano; 2007.
[15] Hocaoglu FO, Gerek ON, Kurban M. Hourly solar radiation forecasting using optimal coefficient 2-D linear filters and feed-forward neural networks. Sol Energy 2008;82(8):714–26.
[16] Mellit A, Kalogirou SA, Shaari S, Salhi H, Arab AH. Methodology for predicting sequences of mean monthly clearness index and daily solar radiation data in remote areas: application for sizing a stand-alone PV system. Renew Energy 2008;33:1570–90.
[17] Cao J, Lin X. Study of hourly and daily solar irradiation forecast using diagonal recurrent wavelet neural networks. Energy Convers Manag 2008;49(6):1396–406.
[18] Reikard G. Prediction solar radiation at high resolutions: a comparison of time series forecasts. Sol Energy 2009;83:342–9.
[19] Cucumo M, Rosa AD, Ferraro V, Kaliakatsos D, Marinelli V. Performance analysis of a 3 kW grid-connected photovoltaic plant. Renew Energy 2006;31(8):1129–38.
[20] Hove T. A method for predicting long-term average performance of photovoltaic systems. Renew Energy 2000;21(2):207–29.
[21] Durisch W, Bitnara B, Mayora JC, Kiessa H, Lamb KH, Closea J. Efficiency model for photovoltaic modules and demonstration of its application to energy yield estimation. Sol Energy Mater Sol Cells 2007;91(1):79–84.
[22] Ayompe LM, Duffy A, McCormack SJ, Conlon M. Validated real-time energy models for small-scale grid connected PV-systems. Energy 2010;35(10):4086–91.
[23] Joyce A, Rodrigues C, Manso R. Modelling a PV system. Renew Energy 2001;22(1):275–80.
[24] De Soto W, Klein SA, Beckman WA. Improvement and validation of a model for photovoltaic array performance. Sol Energy 2006;80:78–88.
[25] Celik AN, Acikgoz N. Modelling and experimental verification of the operating current of mono-crystalline photovoltaic modules using four- and five-parameter models. Appl Energy 2007;84(1):1–15.
[26] Zhou W, Yang H, Fang Z. A novel model for photovoltaic array performance prediction. Appl Energy 2007;84(12):1187–98.
[27] Cameron C, Boyson WE, Riley DM. Comparison of PV system performance-model predictions with measured PV system performance. In: IEEE photovoltaic specialists conference; 2008. p. 33:1–6.
[28] Jones DA, Underwood CP. A modeling method for building integrated photovoltaic power supply. Build Serv Eng Res Technol 2002;23(3):167–77.
[29] Goh TN, Tan KJ. Stochastic modeling and forecasting of solar radiation data. Sol Energy 1977;19:755–7.
[30] Bacher P, Madsen H, Nielsen HA. On-line short-term solar power forecasting. Sol Energy 2009;83:1772–83.
[31] Ashraf I, Chandra A. Artificial neural network based models for forecasting electricity generation of grid connected solar PV power plant. Int J Global Energy 2004;21:119–30.
[32] Sulaiman SI, Abdul Rahman TK, Musirin I. ANN-based technique with embedded data filtering capability for predicting total AC power from grid-connected photovoltaic system. In: International power and engineering and optimization conference; 2008. p. 272–7.
[33] Sulaiman SI, Abdul Rahman TK, Musirin I, Shaari S. Performance analysis of evolutionary ANN for output prediction of a grid-connected photovoltaic system. Int J Electr Comput Eng 2010;5(4):244–9.
[34] Al-Ismaily HA, Probert D. Photovoltaic electricity prospects in Oman. Appl Energy 1998;59:97–124.
[35] Hubbert MK. Nuclear energy and fossil fuels. Am Petrol Inst: Drill Prod Pract 1956:7–25.
[36] Hugh G, Gauch Jr. Fitting the Gaussian curve to ecological data. Ecology 1974;55:1377–81.
[37] Abrams DM, Wiener RJ. A model of peak production in oil fields. Am J Phys 2010;78(1):24–7.
[38] Chow TT, Chan ALS. Numerical study of desirable solar-collector orientations for the coastal region of South China. Appl Energy 2004;79:249–60.
[39] Chow TT, Chan ALS, Fong KF, Lin Z. Some perceptions on typical weather year-from the observations of Hong Kong and Macau. Sol Energy 2006;80(4):459–67.
[40] Yoo SH, Lee ET. Efficiency characteristics of building integrated photovoltaics as a shading device. Build Environ 2002;37(6):615–23.